

Dynamic localization of a charged particle moving under the influence of an electric field

D. H. Dunlap and V. M. Kenkre

Department of Physics and Astronomy, University of New Mexico, Albuquerque, New Mexico 87131

(Received 27 May 1986)

The motion of a charged particle on a discrete lattice under the action of an electric field is studied with the help of explicit calculations of probability propagators and mean-square displacements. Exact results are presented for arbitrary time dependence of the electric field on a one-dimensional lattice. Existing results for the limiting cases of zero frequency and zero field are recovered. A new phenomenon involving the dynamic localization of the moving particle is shown to result in the case of a sinusoidally varying field: The particle is generally delocalized except for the cases when the ratio of the field magnitude and the field frequency is a root of the ordinary Bessel function of order 0. For these special cases it is found to be localized. This localization could be used, in principle, for inducing anisotropy in the transport properties of an ordinarily isotropic material.

I. INTRODUCTION

This paper addresses the motion of a charged particle on a lattice in the presence of an electric field. The analysis is based on exact calculations on discrete lattices. The results are novel and include the onset of a dynamic localization of the moving particle whenever the ratio of the magnitude and the frequency of the electric field has certain values. While the methods we discuss and the results we obtain are applicable in essence to lattices of arbitrary dimensionality, in order to be specific, we begin our considerations with a one-dimensional lattice. We thus consider the motion of a charged particle on a linear chain of sites m ($-\infty < m < +\infty$) under the combined action of a time-dependent electric field in the direction of the lattice and of nearest-neighbor intersite overlap integrals V . The Hamiltonian for the system is

$$H(t) = V \sum_{m=-\infty}^{\infty} (|m\rangle\langle m+1| + |m+1\rangle\langle m|) - eE(t)a \sum_{m=-\infty}^{\infty} m |m\rangle\langle m|. \tag{1.1}$$

In this expression, $|m\rangle$ represents a Wannier state localized on lattice site m , a is the lattice constant, E is the external electric field, and e is the charge on the particle. The nearest-neighbor transfer-matrix element V (overlap integral) has been assumed to be real, and the off-diagonal elements of the position operator x in the Wannier basis have been neglected, i.e., we have assumed that

$$\int_{-\infty}^{\infty} dx \langle m|x\rangle\langle x|(eEx)|x\rangle\langle x|n\rangle = eEam\delta_{m,n}. \tag{1.2}$$

By expressing the particle state $|\psi(t)\rangle$ as a linear combination of Wannier states $|m\rangle$,

$$|\psi(t)\rangle = \sum_m C_m(t) |m\rangle, \tag{1.3}$$

where $C_m(t)$ are the time-dependent amplitudes $\langle m|\psi(t)\rangle$, and by rewriting the quantity eEa as $\mathcal{E}f(t)$,

where \mathcal{E} is constant and $f(t)$ contains the time dependence of the electric field, one obtains from (1.1) the following evolution equation for the amplitudes $C_m(t)$:

$$i dC_m/dt = -\mathcal{E}mf(t)C_m + V(C_{m+1} + C_{m-1}). \tag{1.4}$$

We put $\hbar=1$ throughout this paper.

Our analysis in this paper is based on the exact solution of (1.4) for arbitrary time dependence of $f(t)$ and on the examination therefrom of two observables: the probability propagator $\psi_m(t)$ and the mean-square displacement $\langle m^2 \rangle$. By the probability propagator $\psi_m(t)$ is meant the probability that the particle is at site m at time t , given that it was at site 0 initially. By $\langle m^2 \rangle$ is meant $\sum_m m^2 \psi_m(t)$. When the time dependence of the field is sinusoidal with frequency ω , the self propagator $\psi_0(t)$ generally decays in time, indicating that an initially localized particle becomes delocalized. Correspondingly, the mean-square displacement $\langle m^2 \rangle$ increases without bound. However, for certain critical values of the ratio \mathcal{E}/ω , $\psi_0(t)$ does not decay, $\langle m^2 \rangle$ is bounded, and an initially localized particle therefore remains localized. This is the central result of this paper.

The rest of this paper is set out as follows. In Sec. II, we present our solution of (1.4) for $\psi_m(t)$ and $\langle m^2 \rangle$ for arbitrary time dependence of the electric field and show the onset of dynamic localization in the case of a sinusoidal field. The details of the calculation leading to our solution are presented in the Appendix. Sections III and IV contain, respectively, extensions of our theory to non-nearest-neighbor interactions and to higher dimensions, and concluding remarks.

II. FINAL RESULTS AND DISCUSSION

In solving Eq. (1.4), we first perform a discrete Fourier transform over the site label m by multiplying (1.3) by $\exp(-ikm)$ and summing over all m :

$$C^k(t) = \sum_m e^{-ikm} C_m(t). \tag{2.1}$$

The form of Eq. (1.4) in k space is then

$$\frac{\partial C^k}{\partial t} + (2iV \cos k)C^k = \mathcal{E}f(t)\frac{\partial C^k}{\partial k}. \quad (2.2)$$

The partial differential equation (2.2) can be reduced to a first-order ordinary differential equation by using the method of characteristics.¹ The details of this reduction and of the subsequent solution are in the Appendix. The resulting expression for the probability propagator ψ_m is

$$\psi_m(t) = J_m^2(2V[v^2(t) + u^2(t)]^{1/2}), \quad (2.3)$$

where the quantities u and v are given by

$$u(t) = \int_0^t \cos[\mathcal{E}\eta(t')] dt', \quad (2.4)$$

$$v(t) = \int_0^t \sin[\mathcal{E}\eta(t')] dt', \quad (2.5)$$

$$\eta(t) = \int_0^t f(t') dt'. \quad (2.6)$$

The mean-square displacement corresponding to (2.3) is obtained immediately with the help of the identity² $\sum_m J_m^2(z)m^2 = z^2/2$:

$$\langle m^2 \rangle = 2V^2[u^2(t) + v^2(t)]. \quad (2.7)$$

The principal results (2.3)–(2.7) are valid for any time dependence of the electric field. Of special interest is the case of the sinusoidal field, i.e., $f(t) = \cos\omega t$. For this case u and v are given by

$$u(t) = (1/\omega) \int_0^{\omega t} d\tau \cos[(\mathcal{E}/\omega)\sin\tau], \quad (2.8)$$

$$v(t) = (1/\omega) \int_0^{\omega t} d\tau \sin[(\mathcal{E}/\omega)\sin\tau]. \quad (2.9)$$

Before examining the peculiar behavior of (2.3) and (2.7) with (2.8) and (2.9), it is instructive to recover known results for the case of no field and that of a time-independent (dc) field, respectively. By taking the limit $\omega \rightarrow 0$ in (2.8) and (2.9), we obtain

$$\psi_m(t) = J_m^2((4V/\mathcal{E})\sin(\mathcal{E}t/2)), \quad (2.10)$$

$$\langle m^2 \rangle = 8(V/\mathcal{E})^2 \sin^2(\mathcal{E}t/2). \quad (2.11)$$

The propagator expression (2.10) has been briefly mentioned earlier in the literature on Stark ladders.³ The argument of the Bessel functions in (2.10) is itself an oscillatory function of time, the oscillation frequency being proportional to the magnitude of the electric field. The propagators therefore are oscillatory in time and an initially localized particle remains localized, i.e., does not escape to infinity. It returns to the initial site repeatedly. Equation (2.11) shows this localization explicitly: The mean-square displacement does not grow without bound but oscillates sinusoidally. The argument of the Bessel functions in (2.10) may be written as the product of $2Vt$ with a factor $(\sin z)/z$, where $z = \mathcal{E}t/2$. If we take the limit $\mathcal{E} \rightarrow 0$, i.e., consider particle motion in the absence of an electric field, z vanishes, the multiplicative factor tends to 1, and we recover results known and used widely in the field of excitation dynamics in molecular crystals.⁴

$$\psi_m = J_m^2(2Vt), \quad (2.12)$$

$$\langle m^2 \rangle = 2V^2t^2. \quad (2.13)$$

In this case an initially localized particle does escape to infinity, as is clear both from the decay of the self-

propagator $J_0^2(2Vt)$ and from the fact that the mean-square displacement increases without bound.

We now examine the case of the general sinusoidal electric field and the phenomenon of dynamic localization that it entails. The absence of delocalization in the limit $\omega \rightarrow 0$ discussed above corresponds to the fact that, for that case, $u(t)$ and $v(t)$ have the oscillatory forms $[\sin(\mathcal{E}t)]/\mathcal{E}$ and $[1 - \cos(\mathcal{E}t)]/\mathcal{E}$, respectively. When no field is present, i.e., in the limit $\mathcal{E} \rightarrow 0$, $u(t)$ and $v(t)$ equal t and 0, respectively. For this case, the increase of $u(t)$ without bound leads to delocalization. When neither limit is taken, it is helpful to observe the following important properties of the functions $u(t)$ and $v(t)$. Equations (2.8) and (2.9) show that, whenever ωt equals an integral number n of the period 2π , $u(t)$ equals $[J_0(\mathcal{E}/\omega)]t$ and $v(t)$ vanishes. Furthermore, for general t , the respective differences between u and v and their above special values for $\omega t = 2\pi n$ are both bounded oscillatory functions of time with period $2\pi/\omega$. Their magnitude cannot exceed π/ω . We denote these respective differences by $A_u(t)$ and $A_v(t)$:

$$\begin{aligned} A_u(t) &= u(t) - tJ_0(\mathcal{E}/\omega) \\ &= (1/\omega) \int_0^{\omega t} d\tau \cos[(\mathcal{E}/\omega)\sin\tau] - tJ_0(\mathcal{E}/\omega), \end{aligned} \quad (2.14)$$

$$A_v(t) = v(t) - 0 = (1/\omega) \int_0^{\omega t} d\tau \sin[(\mathcal{E}/\omega)\sin\tau], \quad (2.15)$$

and rewrite the propagator and mean-square displacement expressions (2.3)–(2.7) as

$$\psi_m(t) = J_m^2(2Vt[J_0^2(\mathcal{E}/\omega) + f_1(t)J_0(\mathcal{E}/\omega) + f_2(t)]^{1/2}), \quad (2.16)$$

$$\langle m^2 \rangle = 2V^2t^2[J_0^2(\mathcal{E}/\omega) + f_1(t)J_0(\mathcal{E}/\omega) + f_2(t)], \quad (2.17)$$

$$f_1(t) = 2(A_u/t), \quad f_2(t) = (A_u^2 + A_v^2)/t^2. \quad (2.18)$$

The functions $f_1(t)$ and $f_2(t)$ contain the bounded functions A_u and A_v and therefore decay at large times. The expressions for the propagators and the mean-square displacement are thus dominated by the first term at large times, unless $J_0^2(\mathcal{E}/\omega)$ equals 0. The resulting simplified forms of (2.16),(2.17) for large times are

$$\psi_m(t) = J_m^2(2V^{\text{eff}}t), \quad t \gg 2\pi/\omega, \quad (2.19)$$

$$\langle m^2 \rangle = 2(V^{\text{eff}}t)^2, \quad t \gg 2\pi/\omega. \quad (2.20)$$

Equations (2.19),(2.20) should be compared to (2.12),(2.13) which describe the case of no electric field and consequent delocalization. The only difference between that case and the case of the sinusoidal field represented by (2.19),(2.20) is that in the latter, an effective intersite matrix element V^{eff} appears in place of V . The relation between V^{eff} and V is

$$V^{\text{eff}} = VJ_0(\mathcal{E}/\omega). \quad (2.21)$$

The sinusoidal electric field thus has the effect of reducing the effective velocity or the rate of delocalization of the initially localized particle.

Equation (2.21) shows that the effective intersite interaction vanishes entirely whenever the ratio \mathcal{E}/ω is a root of J_0 . The remarkable result is that, then, the propa-

gators oscillate (do not decay) and the mean-square displacement remains bounded:

$$\psi_m(t) = J_m^2(2V[A_u^2(t) + A_v^2(t)]^{1/2}), \quad (2.22)$$

$$\langle m^2 \rangle = 2V^2[A_u^2(t) + A_v^2(t)]. \quad (2.23)$$

The moving particle is thus effectively localized by the action of the time-dependent electric field. This is the phenomenon of dynamic localization.

Localization under the action of a *time-independent* electric field, as described in (2.10), is perhaps a more familiar effect. It is represented in Fig. 1, where the self-propagator $\psi_0(t)$ is plotted as a function of time for several values of \mathcal{E}/V . As the lowest curve in Fig. 1 shows, the self-propagator decays in the absence of the electric field and the particle escapes [see (2.12)]. But, as the other curves in Fig. 1 show, recurrences are seen for all nonzero values of \mathcal{E}/V and the particle does not escape. The frequency of the recurrences increases with increasing \mathcal{E}/V .

Expected consequences of *time-dependent* electric fields involving no localization can be seen in Fig. 2, where the self-propagator is plotted as a function of time for several values of ω/\mathcal{E} . The lowest curve in Fig. 2 corresponds to the dc field and therefore shows full recurrences as in the upper curves of Fig. 1. However, as the frequency of the field increases from 0, the recurrences are incomplete, the successive peaks in the self-propagator decrease in magnitude, and the particle escapes.

The new result that emerges from our analysis, viz., the phenomenon of dynamic localization, is shown in Figs.

3(a) and 3(b). The self-propagator is plotted in Fig. 3(a) for several values of \mathcal{E}/ω , one of them being 2.405, the first root of J_0 . The corresponding plots of the mean-square displacement are in Fig. 3(b). The behavior depicted in Fig. 2, i.e., decay of ψ_0 , equivalently, escape of the particle, occurs in all the curves of Fig. 3(a), except the one for which $\mathcal{E}/\omega = 2.405$. In this special case, recurrences of the self-propagator show that the particle returns repeatedly to the initially occupied site. This dynamic localization is also evident from Fig. 3(b) where the mean-square displacement is seen to be bounded⁵ only for the special value of \mathcal{E}/ω . Figures 3(a) and 3(b) also show that the phenomenon of dynamic localization disappears for values of \mathcal{E}/ω which are larger than 2.405 as well as smaller than 2.405. The effect returns when \mathcal{E}/ω equals higher roots of J_0 .

III. EXTENSIONS OF THE THEORY

A. Long-range intersite interactions

The extension of our results to a system with long-range intersite interactions is straightforward. If the term $V(C_{m+1} + C_{m-1})$ in (1.4) is replaced by the general expression $\sum_n V_{m-n} C_n$ indicating intersite interactions of arbitrary range, the band energy has the form $2\sum_n V_n \cos nk$ rather than $2V \cos k$. Repeating the calculations detailed in the Appendix for this case then leads to the generalization of the expression (2.7) for the mean-square displacement to

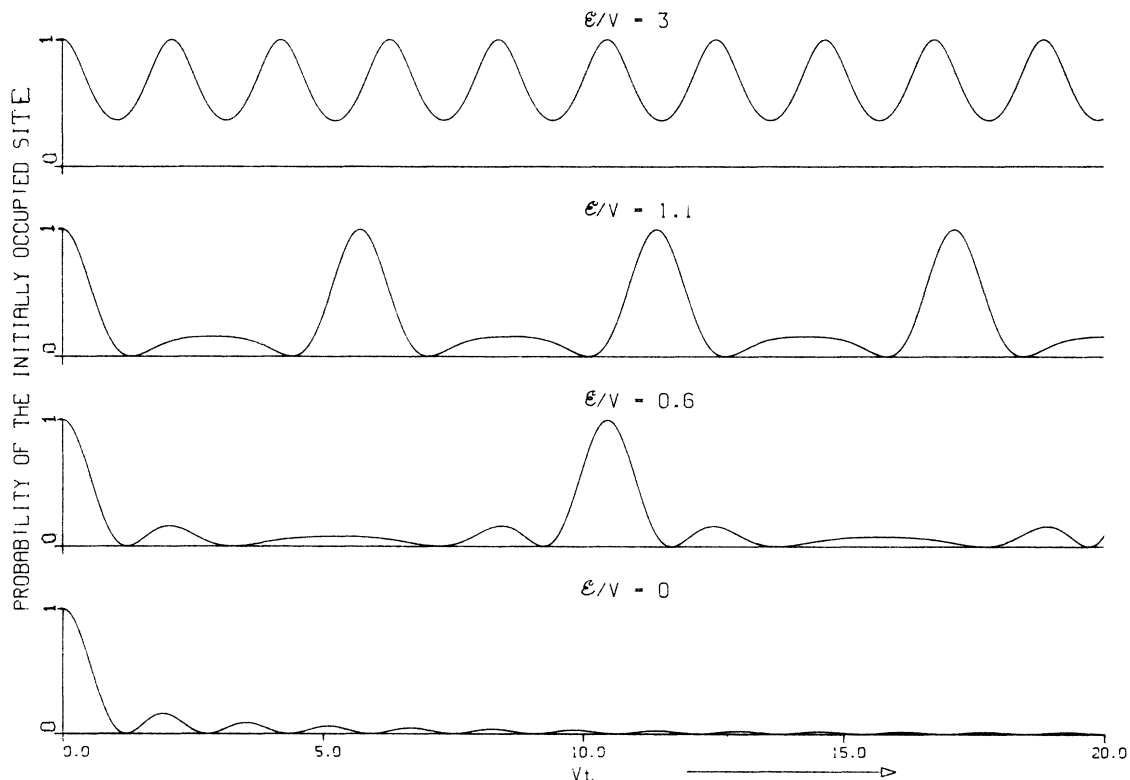


FIG. 1. The self-propagator $\psi_0(t)$, i.e., the probability of the initially occupied site, plotted as a function of the dimensionless time Vt for different values of the ratio \mathcal{E}/V for a dc electric field. The lowest curve shows the decay of $\psi_0(t)$ when $\mathcal{E}/V = 0$. The intermediate values of \mathcal{E}/V cause recurrences of the probability, signifying repeated return of the particle to the initially occupied site.

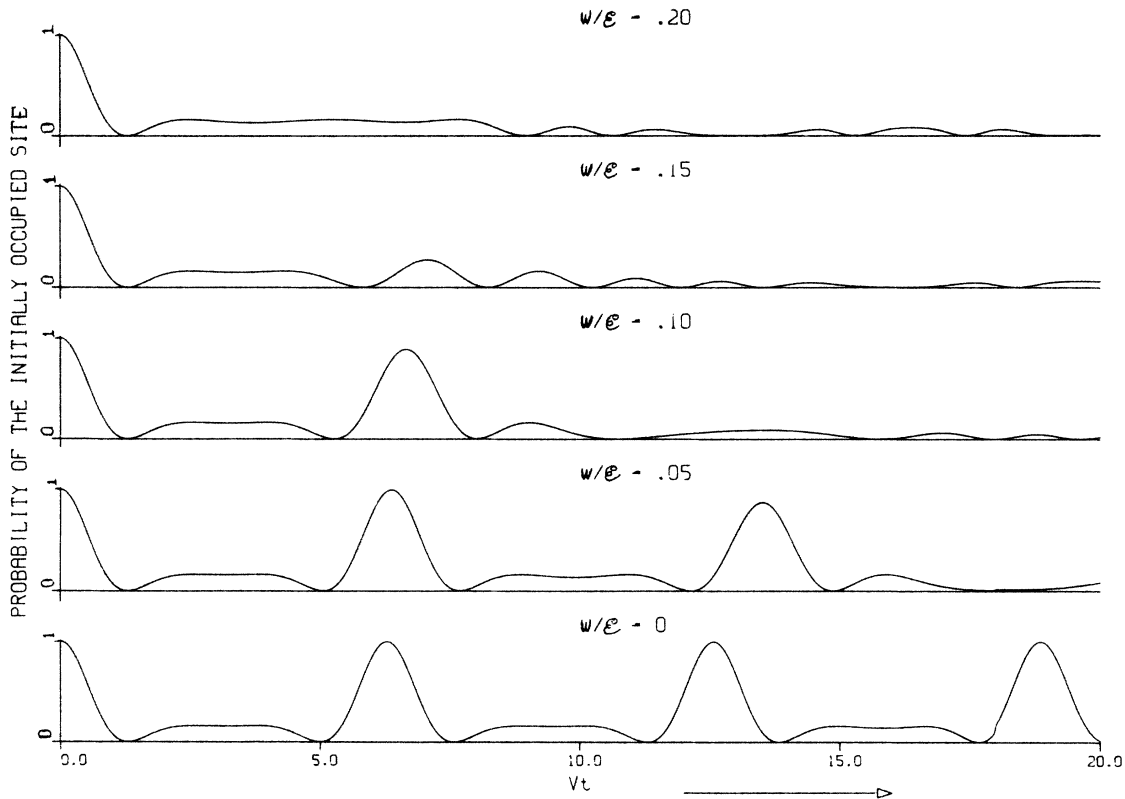


FIG. 2. The self-propagator $\psi_0(t)$, plotted as a function of Vt for different values of the ratio ω/\mathcal{E} for an ac field. The ratio \mathcal{E}/V equals 2 in all cases. Probability recurrences are seen but are incomplete, i.e., the probability of returning to the initially occupied site never reaches unity for nonzero times, for all except the lowest curve, which is the case of the dc field.

$$\langle m^2 \rangle = 2 \sum_n (nV_n)^2 [u_n^2(t) + v_n^2(t)], \quad (3.1)$$

where $u_n(t)$ and $v_n(t)$ are obtained by replacing \mathcal{E} by $n\mathcal{E}$ in (2.8) and (2.9), respectively. Upon substituting the explicit forms of $u_n(t)$ and $v_n(t)$, we get

$$\begin{aligned} \langle m^2 \rangle = 2 \left[\sum_n (nV_n)^2 \right] t^2 \{ J_0^2(n\mathcal{E}/\omega) \\ + 2A_{un}[J_0(n\mathcal{E}/\omega)]/t \\ + (A_{un}^2 + A_{vn}^2)/t \}, \quad (3.2) \end{aligned}$$

where $A_{un}(t)$ and $A_{vn}(t)$, the obvious generalizations of $A_u(t)$ and $A_v(t)$, are also bounded oscillatory functions.

Since the roots of J_0 are not spaced equidistantly on the real line, $J_0(n\mathcal{E}/\omega)$ cannot simultaneously vanish for all n . In other words, dynamic localization in the strictest sense cannot occur in a system with variable range interaction matrix elements. Nevertheless, since V_1 , the nearest-neighbor interaction, is usually dominant in most systems, a significant reduction in the particle mobility will occur when \mathcal{E}/ω is a root of J_0 . A reduction will again occur (but to a less significant extent) when $2\mathcal{E}/\omega$ is a root of J_0 , and again when $3\mathcal{E}/\omega$ is a root, and so on.

B. Higher dimensions

As an extension of the dynamic localization phenomenon to higher dimensions, we consider the motion of a charged particle under the same assumptions as in (1.1) but on a three-dimensional (simple-cubic) lattice rather than on a linear chain. The intersite interactions are assumed to be nearest neighbor and orthogonal so that the motion along each axis is independent of motion along the other two. The probability propagator ψ_{m_x, m_y, m_z} can then be written as the product of three one-dimensional propagators:^{6,7}

$$\psi_{m_x, m_y, m_z}(t) = \psi_{m_x}(t) \psi_{m_y}(t) \psi_{m_z}(t). \quad (3.3)$$

Here, m_x , m_y , and m_z label sites in the x , y , and z directions, respectively.

Because of the separation of the motion along the three axes inherent in (3.3), the generalization of the one-dimensional results is immediate: The form of each of the ψ_{m_r} , where $r = x, y$, or z , is given by the analysis of the one-dimensional case. What enters into the relevant expressions as the magnitude of the electric field is, however, the projection of the field along the axis (r) under consideration. In other words, \mathcal{E} in (2.3) is replaced by the appropriate \mathcal{E}_r , where

$$f(t)\mathcal{E}_r = ea_r \mathbf{E}(t) \cdot \mathbf{r}, \quad (3.4)$$

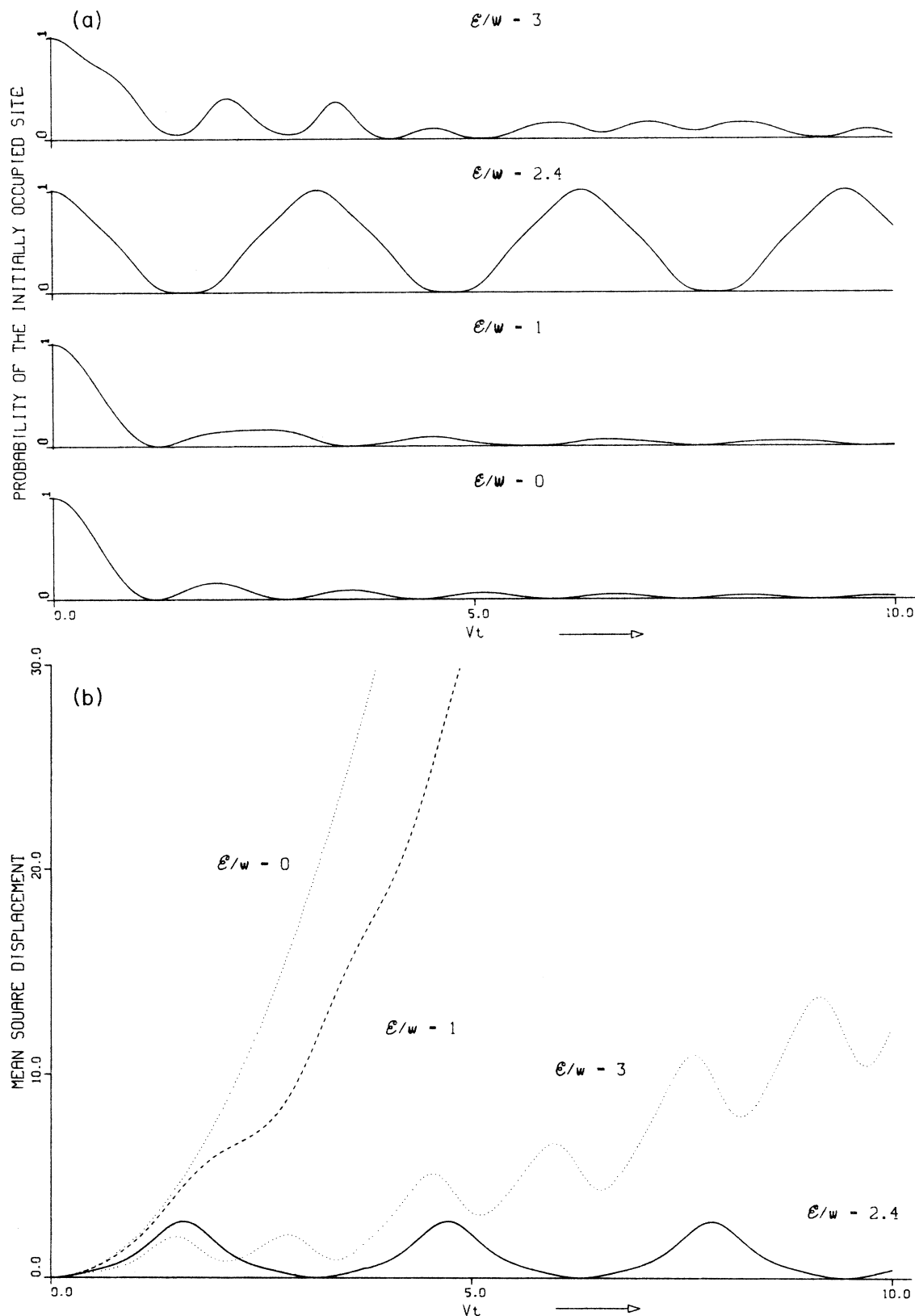


FIG. 3. (a) Dynamic localization exhibited through a plot of the self-propagator $\psi_0(t)$ for different values of the ratio \mathcal{E}/ω . The ratio \mathcal{E}/V equals 2. The field is constant in the lowest curve and time dependent in all the others. With one exception, all the curves for time-dependent fields show a decay of $\psi_0(t)$. The exception corresponds to \mathcal{E}/ω being the first root of J_0 ($\mathcal{E}/\omega = 2.405$) and shows the phenomenon of dynamic localization. (b) Dynamic localization exhibited through a plot of the mean-square displacement $\langle m^2 \rangle$ for the same parameter values as in Fig. 3(a). It is only for the case when \mathcal{E}/ω equals the first root of J_0 that $\langle m^2 \rangle$ remains bounded in time, signifying dynamic localization.

\mathbf{r} being a unit vector along the r axis and a_r the lattice constant along that axis. The generalization of (2.21) valid for the three-dimensional case is simply that the effective matrix element along each axis, V_r^{eff} , is given by (2.19), but with \mathcal{E} replaced by \mathcal{E}_r :

$$V_r^{\text{eff}} = V_r J_0(\mathcal{E}_r/\omega). \quad (3.5)$$

We will consider three special cases to illustrate the new features that the phenomenon of dynamic localization exhibits in higher dimensions: (i) If the field is parallel to the x axis, and \mathcal{E}/ω is a root of J_0 , ψ_{m_y} and ψ_{m_z} will decay in time but ψ_{m_x} will not. An initially localized particle will thus become delocalized in the y - z plane, but remain localized along the x axis. (ii) If the field is in the x - y plane and at an angle of 45° to each of the x and y axes, and $a_r = a$ for all r , then $\mathcal{E}_x = \mathcal{E}_y = \mathcal{E}/2^{1/2}$, and whenever $(\mathcal{E}/2^{1/2})/\omega$ is a root of J_0 , ψ_{m_z} will decay in time but ψ_{m_x} and ψ_{m_y} will not. The particle will be delocalized along the z axis, but will remain bounded in the x - y plane. (iii) If the field has equal projections along all three axes, and $a_r = a$ for all r , then $\mathcal{E}_x = \mathcal{E}_y = \mathcal{E}_z = \mathcal{E}/3^{1/2}$, and the particle will undergo dynamic localization in all three directions whenever $(\mathcal{E}/3^{1/2})/\omega$ is a root of J_0 .

Consider now, for the sake of simplicity, a two-dimensional crystal; i.e., assume V_z to be zero. The particle motion is confined to the x - y plane. In the absence of the electric field, the average speed of the particle along a direction making an angle θ with the x axis is given by $2^{1/2}(V_x^2 a_x^2 \cos^2 \theta + V_y^2 a_y^2 \sin^2 \theta)^{1/2}$. In the presence of the ac field, (3.1) shows that the effective average speed $s(\theta)$ is given by

$$s^2(\theta) = 2[V_x^2 a_x^2 J_0^2(\mathcal{E}_x/\omega) \cos^2 \theta + V_y^2 a_y^2 J_0^2(\mathcal{E}_y/\omega) \sin^2 \theta]. \quad (3.6)$$

In Figs. 4–6 we exhibit explicitly the anisotropic effects which arise as a consequence of dynamic localization by presenting polar plots of the ratio of s to its value s_m in the absence of the field, as a function of \mathcal{E}/ω . We also take $V_x a_x = V_y a_y = Va$. The value of s in a particular direction is displayed as the height of the surface above the origin, and by a polar plot is meant that the quantities plotted along the s_x and s_y axes are $s \cos \theta$ and $s \sin \theta$, respectively. The electric field is directed at 45° to the two axes in Fig. 4, along the y axis in Figs. 5(a) and 5(b), and at 20° to the y axis in Fig. 6.

Figure 4 shows that, when $(\mathcal{E}/2^{1/2}\omega)$ approaches a root of J_0 , the surface shrinks until it becomes a point at the origin, indicating complete absence of motion. In Fig. 5(a) we see surface dimples forming along the s_y axis as \mathcal{E}/ω approaches a root of J_0 . When \mathcal{E}/ω equals the root, the dimples extend to the s_x - s_y origin. They can be seen more clearly in Fig. 5(b), which presents a view from beneath the surface. Figure 6 shows that, as the field magnitude is increased, surface dimples first form along the s_y axis when \mathcal{E}_y/ω is a root of J_0 , and then along the s_x axis when \mathcal{E}_x/ω is a root of J_0 .

IV. CONCLUDING REMARKS

The primary result of this paper is the onset of dynamic localization of a charged particle moving on a discrete lattice under the action of a time-dependent electric field. Our starting point is (1.4), the exact expressions we obtain for the probability of the initially occupied site and for

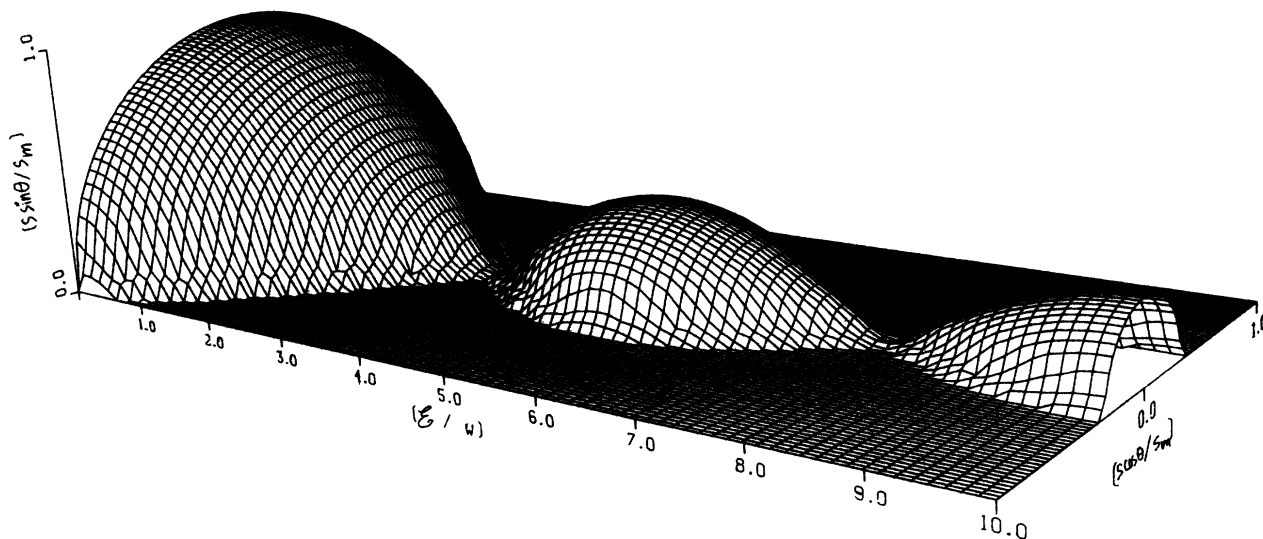


FIG. 4. Anisotropic effects in the motion of the particle arising from dynamic localization induced by a sinusoidal electric field in a two-dimensional crystal [see (3.6)]. Each intersection of the plotted surface with a constant \mathcal{E}/ω plane constitutes a polar plot of the effective average speed $s(\theta)$, normalized to its value $s_m(\theta)$ in the absence of the electric field. The electric field is directed at 45° to the x and the y axes.

the mean-square displacement are (2.3)–(2.9), and our central result is (2.16)–(2.18). Specifically, we have shown that, if the ratio of the electric field energy of the particle, viz., $\mathcal{E} \equiv eEa$ to $\hbar\omega$, where ω is the frequency of the electric field, equals a root of the ordinary Bessel function of order 0, the particle will return repeatedly to

the initially occupied site in a one-dimensional crystal with nearest-neighbor intersite interactions V . We have also shown that the particle will thus be confined⁵ to a region of size smaller than $(2\pi)(V/\hbar\omega)$ times the lattice constant a . Equations (2.22) and (2.23) constitute the explicit statement of this dynamic localization and Figs. 3(a) and 3(b) clarify the effect.

An alternate expression of the localization effect is provided by (2.21) which gives the effective intersite matrix element for the motion of the particle under the action of the sinusoidal electric field and shows that it vanishes when $(eEa/\hbar\omega)$ is a root of J_0 . We have extended the theory to treat interactions which are not necessarily nearest-neighbor (Sec. III A) and to treat dimensions higher than 1 (Sec. III B). Anisotropies induced in the motion of the particle in a two- or three-dimensional crystal are clear from (3.5) and Figs. 4–6. It appears, therefore, that motion in a completely isotropic crystal could be made highly directional simply by the action of a time-dependent field.

The assumptions underlying our treatment include the neglect of the off-diagonal elements of the position operator in the site-localized (Wannier) basis as stated in (1.2), the absence of spatial variations in the electric field, and the neglect of phonon or defect scattering. The first of these is equivalent to the neglect of multiple bands and is justified for electric field magnitudes which are not large enough to cause interband transitions. The second assumption will lose its validity when the characteristic length for the spatial variation of the field is of the order of a lattice constant. Such a situation would arise only for very-high-frequency fields such as in the x-ray range. The third assumption has been made only for simplicity in the present paper. The effect of scattering and the explicit calculation of velocity autocorrelations and thence of the conductivity will form the content of a future publication.

An estimate of the field magnitudes and frequencies required to observe the effect of dynamic localization that we have predicted may be carried out as follows. To avoid the effect being smeared out by collisions, it is expected that the condition $\omega\tau > 1$ should be satisfied, τ being the scattering time. On the other hand, since the first root of J_0 is 2.405, eEa must be more than twice $\hbar\omega$ for dynamic localization to occur. Thus, if the scattering time τ is of the order of 10^{-14} s, the electric field magnitudes required for dynamic localization to occur are in excess of 10^8 V/m, and indeed of the order of 10^9 V/m for a lattice constant of 1 Å. These field magnitudes are larger than typical threshold values for breakdown. We believe this to be the reason the effect has not been observed so far. However, if highly pure crystals are studied at sufficiently low temperatures to cause τ to be of the order of a picosecond or larger, it is conceivable that the effect will be observed for electric fields of the order of 10^6 V/m. Furthermore, there is increased interest in recent times in investigations, both theoretical⁸ and experimental,⁹ which involve extremely strong electric fields, indeed of the order of 10^8 or 10^9 V/m. It is also conceivable that the effects we have predicted will be reflected in spin resonance measurements involving not only electrons but even muons¹⁰ in the presence of strong electric fields.

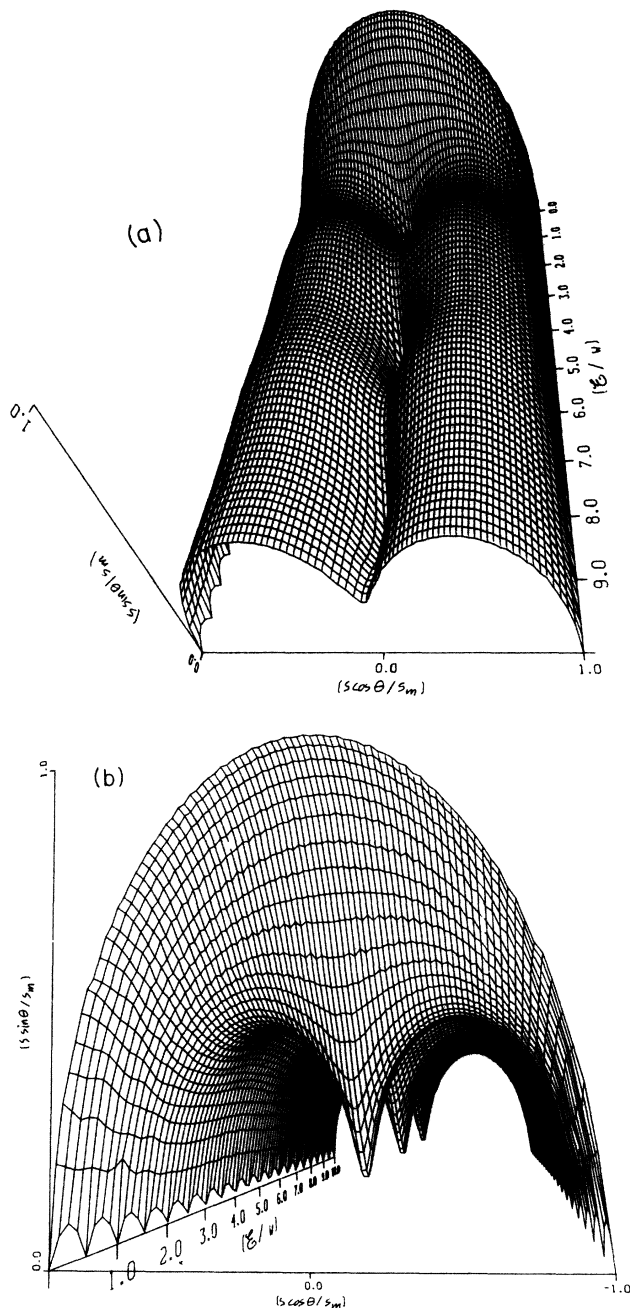


FIG. 5. (a) Anisotropic effects arising from dynamic localization as in Fig. 4. The electric field is directed along the y axis. The points at which dynamic localization occurs manifest themselves as dimples in the surface. (b) The s surface in (a) viewed from a point beneath the surface. The dimples caused by dynamic localization along the y axis are displayed clearly from this perspective as downward pointing spikes.

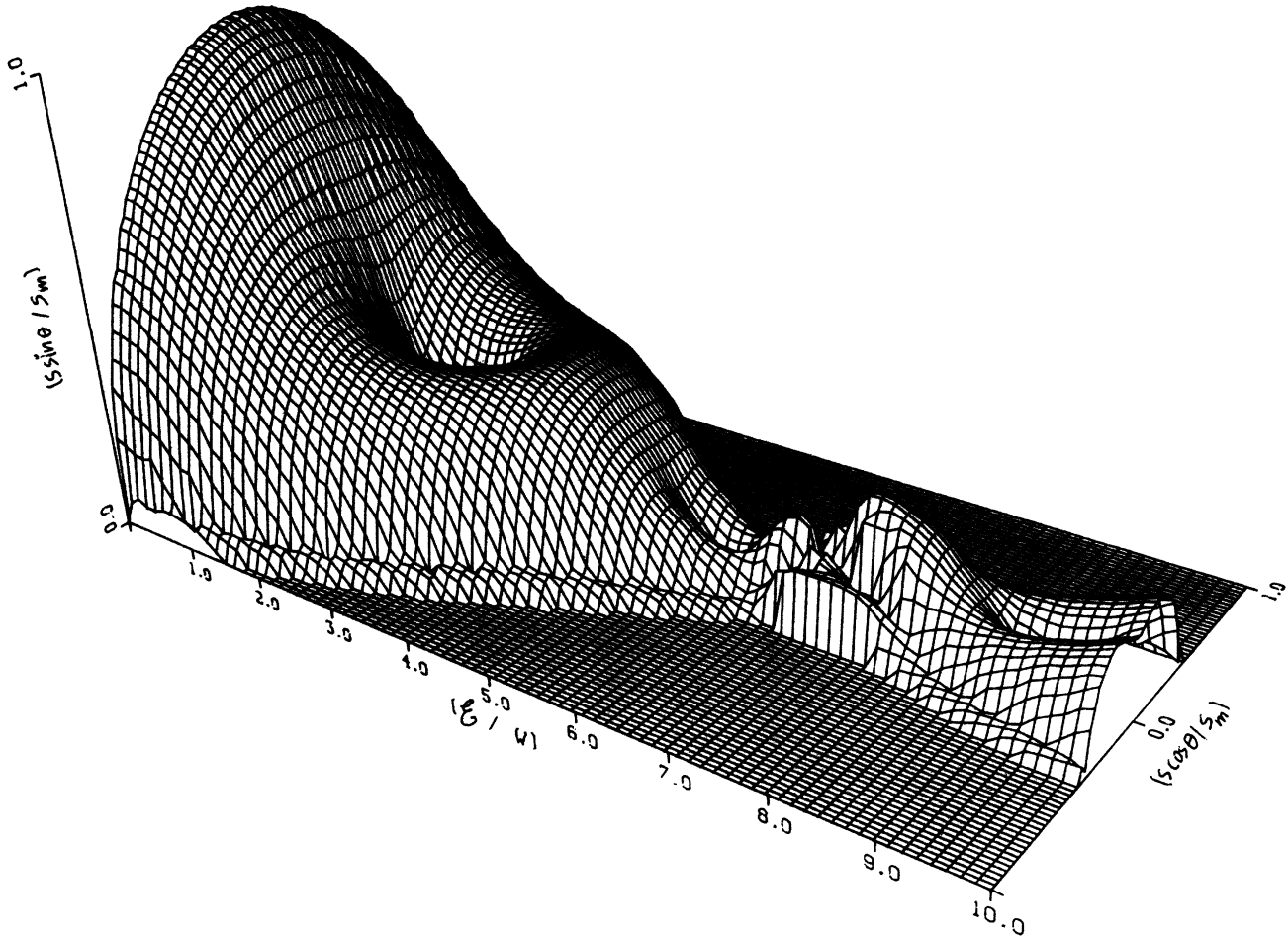


FIG. 6. Anisotropic effects arising from dynamic localization. The electric field is directed at 20° to the y axis. The projections of the field along the two axes being different, dynamic localization does not occur simultaneously along the two axes: It is seen three times along the y axis and only once along the x axis. The result is a highly anisotropic *s* surface.

ACKNOWLEDGMENTS

We thank Dr. Charles Hart for helpful conversations and the National Science Foundation for partial support under Grant No. DMR-85-0638.

APPENDIX

The procedure for obtaining the solution (2.3) to Eq. (2.2) is detailed in this appendix. The method of characteristics¹ allows one to rewrite (2.2) as

$$\frac{dC(s,\tau)}{ds} = -2iV \cos[\tau - \mathcal{E}\eta(s)]C(s,\tau), \tag{A1}$$

with the transformation $s = t$ and $\tau = k + \int ds' f(s') \equiv k + \eta(s)$. The integration of (A1) with constant τ results in

$$C(s,\tau) = C(s=0,\tau) \exp \left[-2iV \int ds' \cos[\tau - \mathcal{E}\eta(s')] \right]. \tag{A2}$$

On transforming back to the original variables, (A2) yields the explicit solution of (2.2):

$$C^k(t) = C^{k+\mathcal{E}\eta(t)} \exp \left[-2iV \int dt' \cos[k + \mathcal{E}\eta(t) - \mathcal{E}\eta(t')] \right], \tag{A3}$$

where by $C^{k+\mathcal{E}\eta(t)}$ is meant the quantity obtained by substituting k by $k + \mathcal{E}\eta(t)$ in the initial (i.e., at $t=0$) C^k . Introducing quantities $\mathcal{U}(t)$ and $\mathcal{V}(t)$ through

$$\mathcal{U}(t) = \int_0^t dt' \cos[\mathcal{E}(\eta(t) - \eta(t'))], \tag{A4}$$

$$\mathcal{V}(t) = \int_0^t dt' \sin[\mathcal{E}(\eta(t) - \eta(t'))], \tag{A5}$$

Eq. (A3) may be rewritten as

$$C^k(t) = C^{k+\mathcal{E}\eta(t)} \exp \{ 2iV [\sin(k)\mathcal{V}(t) - \cos(k)\mathcal{U}(t)] \}. \tag{A6}$$

The use of the identities

$$\exp[-2iV \cos(k)\mathcal{U}(t)] = \sum_n e^{-in\pi/2} e^{ink} J_n(2V\mathcal{U}(t)), \tag{A7}$$

$$\exp[2iV \sin(k)\mathcal{V}(t)] = \sum_n e^{ink} J_n(2V\mathcal{V}(t)), \tag{A8}$$

which express the terms involving $\mathcal{U}(t)$ and $\mathcal{V}(t)$ in terms of ordinary Bessel functions J_m , J_n , etc., and an inverse discrete Fourier transformation, yield directly the following expression for $C_m(t)$:

$$C_m(t) = \sum_r \sum_n C_r(0) e^{ir\mathcal{E}\eta(t)} e^{-in\pi/2} J_n(2V\mathcal{U}(t)) \times J_{m-r-n}(2V\mathcal{V}(t)). \quad (\text{A9})$$

Using Graf's addition theorem for Bessel functions,¹¹ (A9) can be simplified to

$$C_m(t) = \sum_r C_r(0) e^{ir\mathcal{E}\eta(t)} (-\lambda)^{m-r} \times J_{r-m}(2V[\mathcal{V}^2(t) + \mathcal{U}^2(t)]^{1/2}), \quad (\text{A10})$$

$$\lambda = \{[\mathcal{V}(t) - i\mathcal{U}(t)]/[\mathcal{V}(t) + i\mathcal{U}(t)]\}^{1/2}. \quad (\text{A11})$$

Finally, the probability propagator $\psi_m(t)$, which is merely $|C_m|^2$, is given from (A10) as

$$\psi_m(t) = J_m^2(2V[\mathcal{V}^2(t) + \mathcal{U}^2(t)]^{1/2}). \quad (\text{A12})$$

It is possible to further simplify (A12) by noticing that $\mathcal{V}^2(t) + \mathcal{U}^2(t)$ is exactly equal to $v^2(t) + u^2(t)$, where

$$v(t) = \int_0^t \sin[\mathcal{E}\eta(t')] dt', \quad (\text{A13})$$

$$u(t) = \int_0^t \cos[\mathcal{E}\eta(t')] dt'. \quad (\text{A14})$$

Equation (A12) is then reduced to (2.3).

¹A. N. Tikhonov, A. B. Vasil'eva, and A. G. Sveshnikov, *Differential Equations* (Springer-Verlag, Munich, 1980).

²I. S. Gradshteyn and I. M. Ryzhik, *Table of Integrals, Series, and Products*, 4th ed. (Academic, New York, 1965), p. 980.

³H. Fukuyama, R. A. Bari, and H. C. Fogedby, *Phys. Rev. B* **8**, 5579 (1973).

⁴See, e.g., V. M. Kenkre, in *Energy Transfer Processes in Condensed Matter*, edited by B. Di Bartolo (Plenum, New York, 1984), p. 205.

⁵Since the magnitude of A_u and A_v cannot exceed π/ω , (2.20) shows that the mean-square displacement is bounded by $(2\pi V/\omega)^2$.

⁶A. A. Maradudin, E. W. Montroll, and G. H. Weiss, *Solid*

State Physics, Suppl. 3: Theory of Lattice Dynamics in the Harmonic Approximation (Academic, New York, 1963), p. 150.

⁷V. M. Kenkre, *Z. Phys. B* **43**, 221 (1981); A. Fort, V. Ern, and V. M. Kenkre, *Chem. Phys.* **80**, 205 (1983).

⁸C. L. Roy and P. K. Mahapatra, *Phys. Rev. B* **25**, 1046 (1982).

⁹S. Maekawa, *Phys. Rev. Lett.* **24**, 1175 (1970).

¹⁰K. W. Kehr, D. Richter, J. M. Welter, O. Hartmann, E. Karlsson, L. O. Norlin, T. O. Niinikoski, and A. Yaouanc, *Phys. Rev. B* **26**, 567 (1986).

¹¹*Handbook of Mathematical Functions*, edited by M. Abramowitz and I. A. Stegun (Dover, New York, 1965), p. 363.

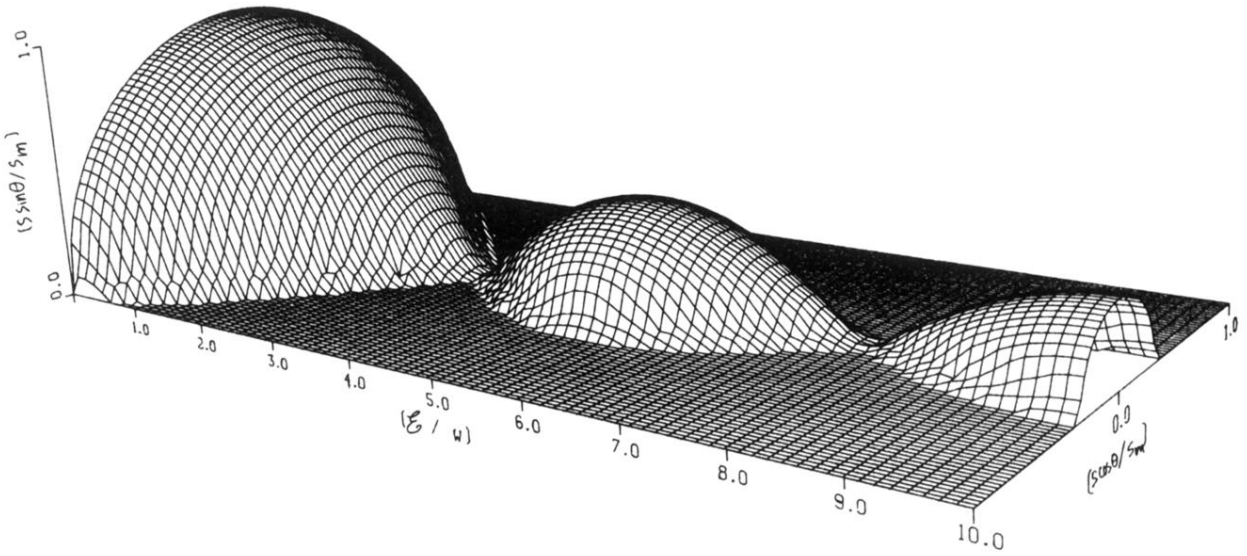


FIG. 4. Anisotropic effects in the motion of the particle arising from dynamic localization induced by a sinusoidal electric field in a two-dimensional crystal [see (3.6)]. Each intersection of the plotted surface with a constant E/ω plane constitutes a polar plot of the effective average speed $s(\theta)$, normalized to its value $s_m(\theta)$ in the absence of the electric field. The electric field is directed at 45° to the x and the y axes.

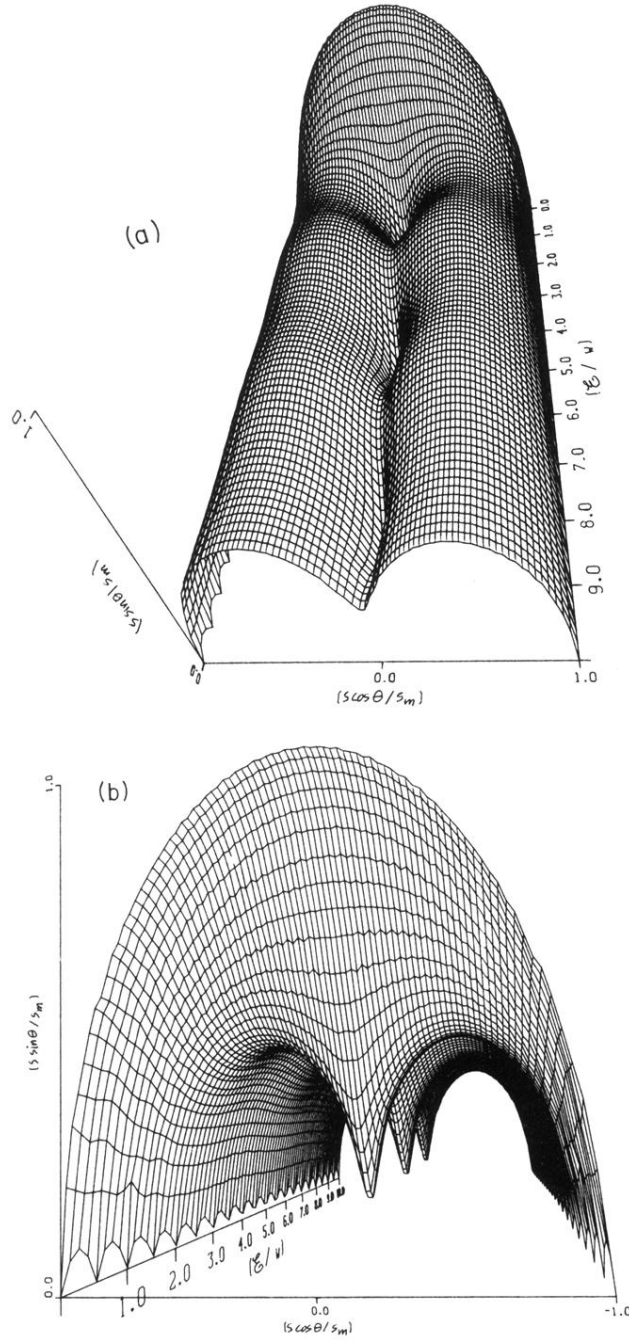


FIG. 5. (a) Anisotropic effects arising from dynamic localization as in Fig. 4. The electric field is directed along the y axis. The points at which dynamic localization occurs manifest themselves as dimples in the surface. (b) The s surface in (a) viewed from a point beneath the surface. The dimples caused by dynamic localization along the y axis are displayed clearly from this perspective as downward pointing spikes.

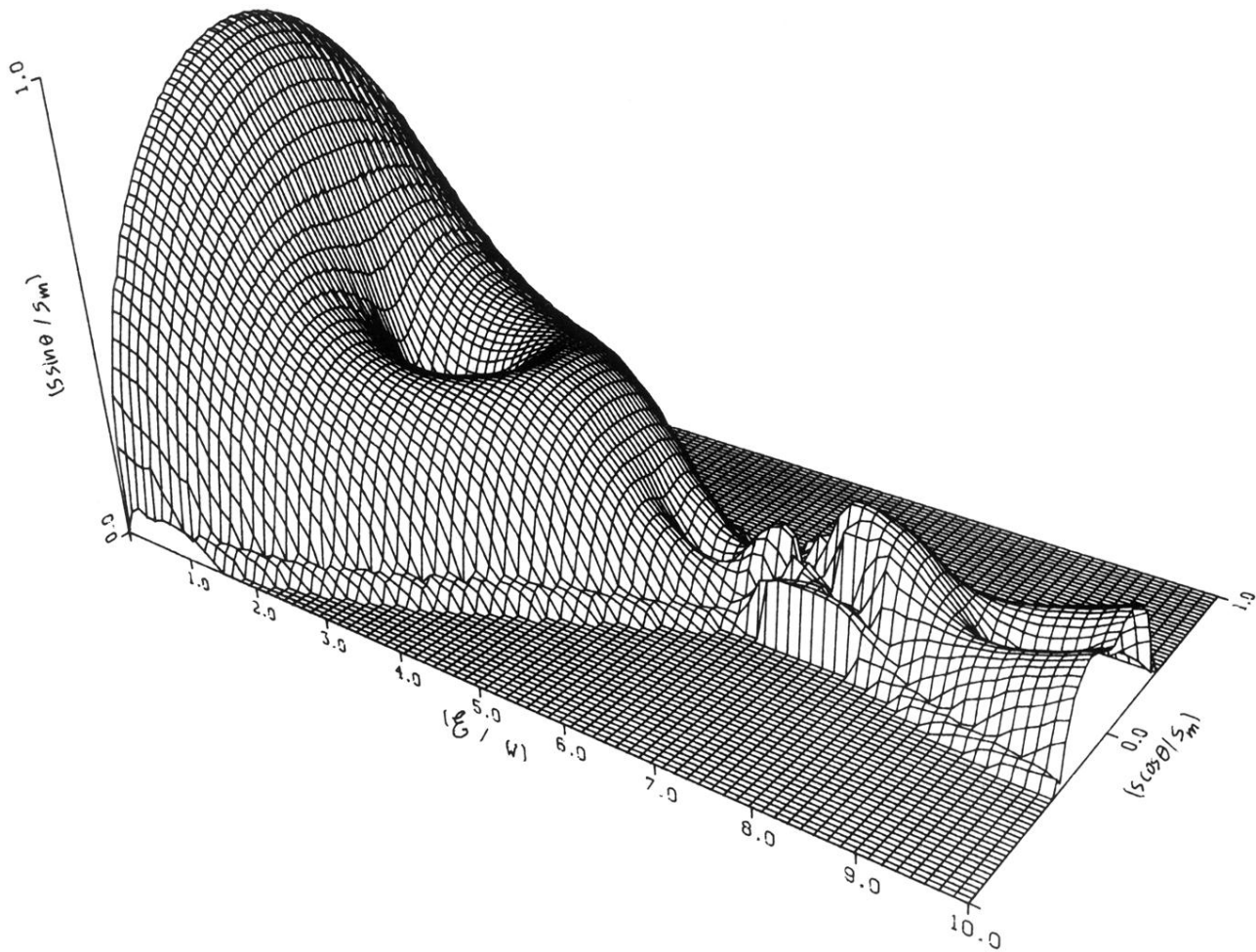


FIG. 6. Anisotropic effects arising from dynamic localization. The electric field is directed at 20° to the y axis. The projections of the field along the two axes being different, dynamic localization does not occur simultaneously along the two axes: It is seen three times along the y axis and only once along the x axis. The result is a highly anisotropic s surface.